

Preparation of Novel Fe Catalysts from Industrial By-Products: Catalytic Wet Peroxide Oxidation of Bisphenol A

Riikka Juhola,¹

Anne Heponiemi,¹ 

Email anne.heponiemi@oulu.fi

Sari Tuomikoski,¹

Tao Hu,¹

Tuomas Vielma,²

Ulla Lassi,^{1,2}

¹ Research Unit of Sustainable Chemistry, University of Oulu, P.O. Box 3000, 90014 Oulu, Finland

² Kokkola University Consortium Chydenius, University of Jyväskylä, P.O. Box 567, 67701 Kokkola, Finland

Abstract

Biomass-based carbon residue (CR) was used as a support material for iron catalysts to degrade bisphenol A (BPA) in catalytic wet peroxide oxidation (CWPO). According to the results, CR and Fe/CR catalysts are suitable materials for CWPO. The Fe catalysts were prepared by either incipient wet impregnation or wet impregnation methods with an iron chloride solution. The specific surface area of the prepared catalysts was 17–91 m² g⁻¹, and it remained the same after the oxidation experiments. The CWPO experiments were carried out batch-wise at c(BPA) = 60 mg L⁻¹, c(H₂O₂) = 1.5 g L⁻¹, c(catalyst) = 1–2 g L⁻¹, T = 50 °C and at the initial pH. The 5.0Fe/CR catalyst

was found to be active with BPA removal and total organic carbon (TOC) conversion of 83 and 64%, respectively, and was the most stable catalyst with negligible iron leaching during the 3 h experiment.

Keywords

Bisphenol A

Catalytic wet peroxide oxidation (CWPO)

Fe-catalyst

Biomass

1. Introduction

The world's freshwater resources continue to deteriorate due to pollution and climate change. In many countries, such as India [1], the Netherlands [2] and Finland [3], the aquatic environment has been found to contain trace levels ($\mu\text{g L}^{-1}$ or ng L^{-1} or even lower) of various pollutants, including industrial compounds, personal care products, endocrine-disrupting chemicals (EDCs) etc. [4, 5, 6]. These compounds enter the aquatic environment from industrial and municipal effluents [7] because the existing wastewater treatment plants (WWTPs) were designed to remove mainly inorganic substances, nutrients and pathogens, not trace levels of organic refractory compounds [8]. Therefore, more efficient water treatment methods and sustainable water reuse technologies are needed.

Bisphenol A (2,2-bis(4-hydroxyphenyl)propane, BPA), classified as an EDC by the U.S. Environmental Protection Agency [9], is one of the compounds found in various bodies of water [10, 11]. BPA is a synthetic organic substance that has been mainly used to produce polycarbonate plastics and epoxy resins [12]. Other applications include thermal paper, paper coatings and building materials [13]. BPA has been rated a high-volume production chemical with a global production rate of more than 5 Mt in 2015 [14]. According to the U.S. EPA [9], more than 1 million pounds of BPA leaches into U.S. environment every year. Several studies have shown that BPA has harmful effects on animals due to estrogenic activity, such as inducing feminization [15]

and by disruption of the development of the reproductive system [16, 17]. To date, various techniques have been implemented to treat BPA, including ozonation [18], Fenton/photo-Fenton [19, 20, 21] and adsorption [22]. Ozonation has high oxidation potential in the degradation of BPA, but the process is not economical due to the high operational costs [23]. Fenton/photo-Fenton is an economical treatment method, but the optimal reaction conditions are limited to a pH of less than 4, and the process produces iron-containing sludge as secondary waste [24]. The adsorption process is highly effective and easily conducted, but it also produces secondary waste. The adsorbent has to be regenerated or treated with another technique, which increases the operational costs [25].

Compared to these purification technologies, catalytic wet peroxide oxidation (CWPO) has shown excellent removal efficiency for several organic compounds, such as phenol, carboxylic acids and industrial effluents [26, 27, 28, 29, 30, 31]. CWPO was adapted from a classical Fenton process [32], which has been referred to as an economical alternative to wastewater treatment techniques [33] because it requires only basic equipment and operates at ambient-like pressure and temperature [34, 35]. During this process, hydrogen peroxide (H_2O_2) decomposes in the presence of the catalyst (typically Fe or Cu salts) producing highly reactive hydroxyl radical species (OH^\cdot) that degrade most of the organic pollutants present in the wastewater [36]. Compared to the traditional Fenton process, CWPO can be conducted over a broad pH range by using heterogeneous catalysts [37]. Improvements, especially in finding an optimal catalyst, would make this technique even more efficient, and materials, such as pillared clays [38], silica and alumina [39], have been tested in CWPO. In recent years, carbon-supported metal catalysts have interested many researchers as carbon materials have been found to possess unique properties, such as good stability under acidic and basic conditions and a high specific surface area that leads to highly dispersed metal phases [40, 41]. According to the literature to date, only a few studies have used carbon-based catalysts in the CWPO process [42], but the studies showed very promising results in this field of study. Many of these studies were conducted by using commercial activated carbons [43, 44, 45, 46]; however, environmentally friendly alternatives that are more cost-

effective are needed. Industrial processes generate various waste materials and by-products, and all utilization applications are preferred to landfilling. Moreover, within the European Union (EU) region, legislation restricts the landfilling of waste materials that contain more than 10% organic carbon [47]. Therefore, an alternative use for waste materials, such as recycling, has to be found. Although there has been interest in using the carbon-based waste materials in different types of wastewater treatment applications, such as adsorption [48, 49, 50], only a few studies in the literature focused on the preparation of carbon-supported catalysts from waste material in CWPO. In the present study, in which waste material formed during the biomass gasification process, carbon residue (CR) was used as a carbon-based catalyst support. Carbonaceous materials are known to contain metal impurities such as iron and their presence may increase the catalytic activity [51]. Also, the impregnated iron has been shown to enhance the catalytic oxidation of various compounds using carbon-based catalyst in CWPO in several works [35, 52, 53, 54, 55, 56]. Therefore iron was chosen as an active metal for the CR support.

The objective of this study was to investigate CWPO of BPA using a biomass-based CR as a support for iron catalysts. Iron was incorporated on the CR by incipient wet impregnation or wet impregnation. The physical and chemical states of the prepared catalysts were characterized with inductively coupled plasma optical emission spectroscopy (ICP-OES), Brunauer-Emmet-Teller (BET) equations, X-ray diffraction (XRD), diffuse reflectance infrared Fourier transform spectroscopy (DRIFTS), and field emission scanning electron microscopy (FESEM). The CWPO results were analyzed in terms of BPA removal and total organic carbon (TOC) conversion using high-performance liquid chromatography (HPLC) and TOC analytical techniques, respectively. The possible leaching of active iron from the catalysts was determined with ICP-OES. Kinetics and by-products were also evaluated.

2. Experimental

This section presents the characterization techniques and analytical methods carried out to determine the physical and chemical state of the

fresh and used catalysts, as well as to assess the activity and stability of the prepared iron catalysts in catalytic wet peroxide oxidation.

2.1. Materials

The CR used in this study was waste material obtained from a pilot-scale biomass gasification plant (Sievi, Finland) that involved a 150 kW airblown downdraft gasifier operating at a temperature of about 1000 °C. Finnish wood biomass was used as fuel for the gasifier. Based on previous studies, the carbon residue contained soluble nutrients. The main components were calcium (42.3 g kg⁻¹) and sodium (71 mg kg⁻¹). In addition, the CR also contained metals, for example, copper (130 mg kg⁻¹) and zinc (134 mg kg⁻¹). The pH of the material was 9, the total carbon content 15%, the specific surface area 15 m² g⁻¹, the pore size 16 nm and the pore volume 0.06 cm³ g⁻¹. The detailed properties of the material are presented elsewhere [57].

Before use, the carbon residue was dried at 105 °C to achieve constant weight and then further ground and sieved so the particles were smaller less than 150 µm. The CR was thoroughly washed using deionized (DI) water until neutral pH was reached, dried again at 105 °C overnight and stored in a desiccator. The chemicals, including ferric chloride (≥98%, Merck), bisphenol A (≥99%, Sigma–Aldrich), hydrogen peroxide (30% w/w, Merck), hydrochloric acid (0.09983 ± 0.00041 mol L⁻¹, FF-Chemicals) and sodium hydroxide (0.09992 ± 0.0073 mol L⁻¹, FF-Chemicals), were reagent grade. Commercial activated carbon Norit (AC Norit, Norit®GAC 1240 Plus) from coconut peel was used as a reference material.

2.2. Preparation of the Catalysts

Three iron-loaded carbon residue-derived catalysts (Fe/CR) were prepared by either incipient wet impregnation or wet impregnation to the CR with an aqueous solution of ferric chloride. The Fe concentrations were adjusted to obtain 2.5, 5.0 and 33% Fe content (w/w) on the catalyst, and the corresponding catalysts were thus named 2.5Fe/CR, 5.0Fe/CR and 33Fe/CR, respectively.

The multi-step method presented by Chang et al. [44] was used to impregnate the CR with iron (2.5Fe/CR). After the incipient impregnation, the mixture was stirred for 16 h at room temperature and at initial pH. Then, the 2.5Fe/CR catalyst was separated from the liquid phase and dried at 105 °C overnight. These steps were repeated five times in order to achieve higher iron content and stability for the 2.5Fe/CR catalyst.

For the 5.0Fe/CR and 33Fe/CR catalysts, a one-step method for iron wet impregnation was performed. In the preparation of the 5.0Fe/CR catalyst, 8 mL of DI water per gram of CR and 8 mL of 1 M sodium hydroxide were added to the Fe/CR mixture to increase the pH to 8–9 and to form ferric hydroxide. The 33Fe/CR catalyst was prepared by adjusting the pH from initial 2–2.5 to neutralize only part of the FeCl₃ solution. After the pH was adjusted, the suspensions were slowly evaporated using a rotating evaporator at 40–50 °C under reduced pressure and further dried at 105 °C overnight.

After impregnation, the dried catalysts were ground and sieved to ensure the particles were smaller less than 150 µm. Finally, the catalysts were calcined in a furnace at 280 °C for 5 h under nitrogen gas flow (15 L min⁻¹).

2.3. Catalyst Characterization

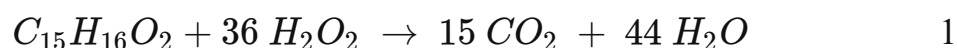
The iron content of the fresh and used catalysts was measured with ICP-OES (Perkin Elmer Optima 5300 DV). Sorption–desorption isotherms of nitrogen at –196 °C were used to determine specific surface areas and pore volumes of the carbon products using the Micrometrics ASAP 2020 instrument. The specific surface areas and the pore volumes were calculated using BET and Barrett–Joyner–Halenda (BJH) equations, respectively. Powder XRD patterns for the phase identification of iron on the catalysts were obtained using the PANalytical X’pert Pro diffractometer system with the Cu K α ray at 45 kV and 40 mA ($\lambda = 1.5406$ Å). Diffractograms were collected in the 2θ range from 5° to 80° using a scan speed of 0.019°/s. The diffractograms were compared to the Powder Diffraction File standards from the International Centre for Diffraction DATA (ICDD). The diffuse reflectance mode was used to

record the DRIFTS (Brüker PMA 50 Vertex 80V) of the AC, CR and Fe/CR catalysts to identify the possible functionality of these samples. The baseline was measured with KBr, which was also used for the dilution of the samples (1:100). In each experiment, the sample chamber was purged with nitrogen (100 mL min⁻¹), continuously heated at a rate of 10 °C per minute to the target temperature (105 °C) and maintained at that temperature for 1 h. Measurements were obtained in the range of 400–4000 cm⁻¹ with a resolution of 4 cm⁻¹ and 100 scans per minute. The surface morphology of the fresh and used Fe/CR catalysts was investigated using a Zeiss ULTRA plus FESEM combined with energy-dispersive X-ray spectroscopy (EDS) for element mapping.

2.4. Catalytic Wet Peroxide Oxidation of BPA and Kinetic Measurements

The catalysts were studied in the catalytic wet peroxide oxidation of BPA aqueous solution . Please take the full stop and enter off.

(60 mg L⁻¹). The amount of hydrogen peroxide needed for complete mineralization of the organic carbon was estimated to be 5.6 times the mass ratio of H₂O₂/BPA using the following reaction (Eq. 1):



The oxidation reaction was carried out in a three-necked 500 mL round bottom flask, equipped with a magnetic stirrer and a reflux condenser, and the reactor was placed in a water bath. The powdered catalyst or carbon residue (1 or 2 g L⁻¹) was introduced into 160 mL of an aqueous BPA solution (60 mg L⁻¹) under continuous stirring. The experiments were run at 50 °C and the initial pH for 3 h. After the temperature was stabilized, a solution of 0.15% H₂O₂ was added to the reactor, which was taken as the starting point of the reaction (t = 0). H₂O₂ was added during the experiment as doses (1.5 g L⁻¹) so that the stoichiometric amount of the H₂O₂/BPA ratio was achieved. Samples of the reaction medium were taken periodically and filtered through 0.45 µm filter paper. Dissolved oxygen content and pH (Hach Lange HQ40d portable meter, LDO and pH probes) were followed during the experiment. To study the possible adsorption of BPA on the catalyst surface, adsorption

experiments were performed in the same reaction conditions without adding the oxidizing agent, H_2O_2 .

2.5. Analytical Methods

The bisphenol A concentration and the oxidation by-products were identified and quantified with HPLC equipped with an ultraviolet–visible (UV–Vis) detector, using a 226 nm wavelength (Shimadzu SPD-10A). The mixture of acetonitrile (ACN, 45%) and formic acid (FA, 0.1%) were used as the eluent (flow rate 0.5 mL min^{-1}), and the compounds was separated with the SunFire™ C18 5 m $2.1 \times 100 \text{ mm}$ column, operated at a temperature of 40°C . Mineralization of the TOC in the wastewater and in the BPA samples was monitored by using the Skalar ~~Formaes~~ Formacs^{HT} Total Organic Content/Total Nitrogen analyzer. In this system, all organic and inorganic carbon in the sample was catalytically oxidized at $750\text{--}950^\circ\text{C}$ to gaseous carbon dioxide. CO_2 was detected with a non-dispersive infrared detector at a wavelength of $4.2 \mu\text{m}$. The inorganic carbon content of the sample was measured with acidic oxidation, and the TOC of the sample was determined by subtracting the inorganic carbon content from the total carbon content. The amount of possible leached iron after the oxidation reactions was determined with an atomic absorption spectrophotometer (AAS, PerkinElmer AAnalyst 200) instrument, at a wavelength of 248.3 nm .

AQ1

3. Results and Discussion

3.1. Characterization of the Fresh Catalysts

The iron content (determined with ICP-OES), together with the textural characteristics of the fresh catalysts, is presented in Table 1. In the case of the 5.0Fe/CR catalyst, prepared in basic conditions (pH 8–9), the iron content was in good agreement with the target value. The addition of iron per repetition to the 2.5Fe/CR catalyst was 2.5 wt% at each repetition; that is, the theoretical amount of Fe on the support should have been 12.5 wt%. However, the total amount of impregnated iron was 5.0 wt%. Compared to results reported by Chang et al. [44] who used the same method, the difference might be because the carbon

material was different. Furthermore, during the repetitions, part of the impregnated iron might have been re-dissolved into the liquid phase and some support material lost during the separation steps. Catalytic activity is related more to the high metal content than to the surface area [58], which was why a catalyst containing 33 wt% of iron was prepared. However, the iron content of that catalyst was 14 wt%. As previously described, it is difficult to obtain high amounts of impregnated iron inside CR in one step. It has been reported that high iron content in the mixture produced a carbon with a smaller surface area [59]. The lack of impregnated iron might be because that there was not enough available surface area on the CR support.

Table 1

Iron content, BET surface area, total pore volume and relative distribution of micro-, meso- and macropores of fresh catalysts

Catalyst	Fe-content (%)	BET surface area (m² g⁻¹)	Total pore volume (cm³ g⁻¹)	V_{Micro} (%)	V_{Meso} (%)	V_{Makro} (%)
2.5Fe/CR	5.0	62.8	0.096	5.66	77.9	16.4
5.0Fe/CR	4.0	66.0	0.091	6.78	74.9	18.3
33Fe/CR	14	17	0.074	1.11	46.8	52.1
AC	0.21	923	0.434	13.3	13.9	73.6
CR	0.20	91.3	0.119	6.89	76.6	16.5

According to the results presented in Table 1, the surface area of the carbon residue was 91.3 m² g⁻¹. All the iron loaded catalysts showed that the surface area and the pore volume decreased with the increase in iron. This variation may indicate that the ferric species was immobilized in the pores of the CR, leading to a reduction in the surface area. In addition, the higher iron content in the 33Fe/CR catalyst led to a significantly lower surface area. These results are in line with those presented in the literature [60, 61]. The surface area and the total pore volume were significantly higher in the reference material, commercial activated carbon (AC Norit).

X-ray diffractograms of the powdered carbon residue support and Fe catalysts are presented in Fig. 1. The strong sharp peaks in the prepared 33Fe/CR catalyst suggest good crystallinity of iron oxide. The major peaks for the 33Fe/CR catalyst matched well with the crystalline iron species of hematite (Fe_2O_3 , the main peaks were at 2θ at 31.7° , 33.1° , 35.6° , 45.4° and 56.4° , JCPDS: 01-089-0597). For comparison, the reflections obtained for the 2.5Fe/CR catalyst at 2θ 26.6° and 35.5° corresponded to iron carbonate (JCPDS: 01-080-2679) whereas no iron was detected in the XRD pattern of the 5.0Fe/CR catalyst. Instead, the reflections obtained for the 5.0Fe/CR catalyst were found to be a match for sodium chloride (JCPDS: 01-076-3452). This result is reasonable as the used CR support had been found to contain soluble nutrients, such as sodium [57]. The NaCl content was further verified with EDS analysis, which indicated the presence of sodium (3.3 wt%) and chlorine (6.7 wt%). However, according to ICP-OES (Table 1), the 5.0Fe/CR catalyst contained iron. Again, this result was confirmed with the EDS analysis, which showed 7.4 wt% of iron. Therefore, it might be possible that the probable small ferric oxo-hydroxide particles formed during the basic environment were precipitated in the macropores, not on the outer surface of carbon, and consequently could not be detected with XRD [38]. In addition, it was noticed that four peaks of Fe_2O_3 are overlapped with NaCl peaks at 2θ value of (27.3° , 31.7° , 45.4° and 66.2°) (Fig. 2). The presence of NaCl might also explain the lower iron content of this particular catalyst (Table 1). Furthermore, the reflection pattern for the carbon residue support was obtained at 2θ 26.6° , 29.4° , 32.9° , 39.4° , 43.1° and 47.4° , corresponding to calcium carbonate (JCPDS: 01-078-3262). This was due to the high Ca content of the carbon residue [57].

Fig. 1

X-ray diffractograms of the fresh carbon residue support (1) and Fe catalysts (2–4). (*plus*) JCPDS:01-078-3262 (CaCO_3); (*asterisk*) JCPDS: 01-076-3452 (NaCl); (*double quotes*) JCPDS: 01-080-2679 (FeCO_3); (*hash*) JCPDS: 01-089-0597 (Fe_2O_3)

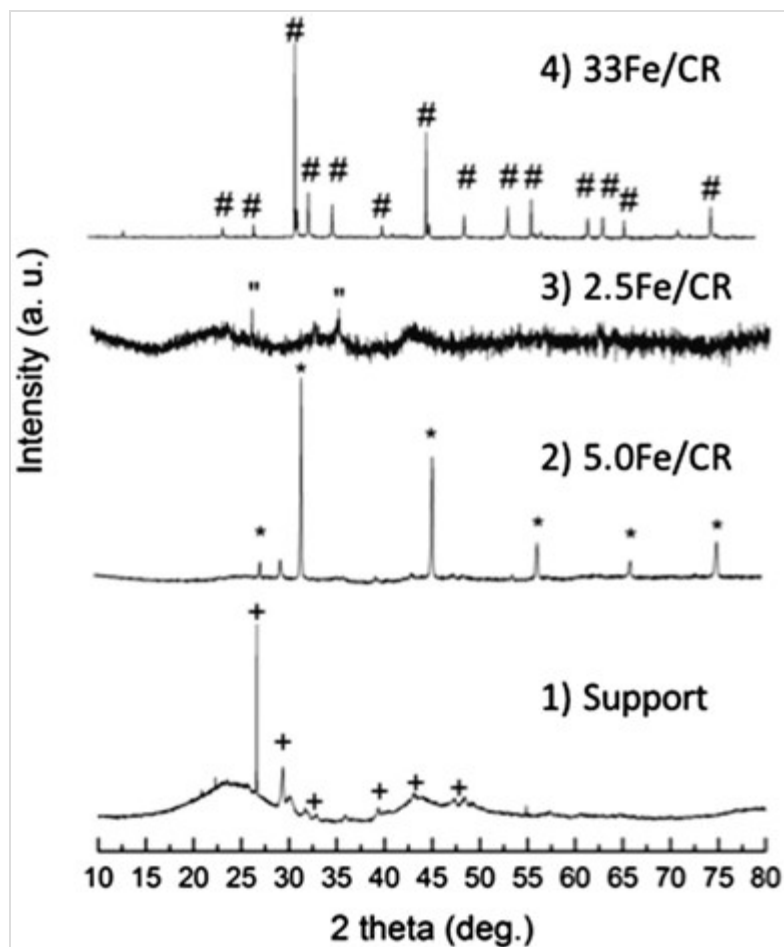
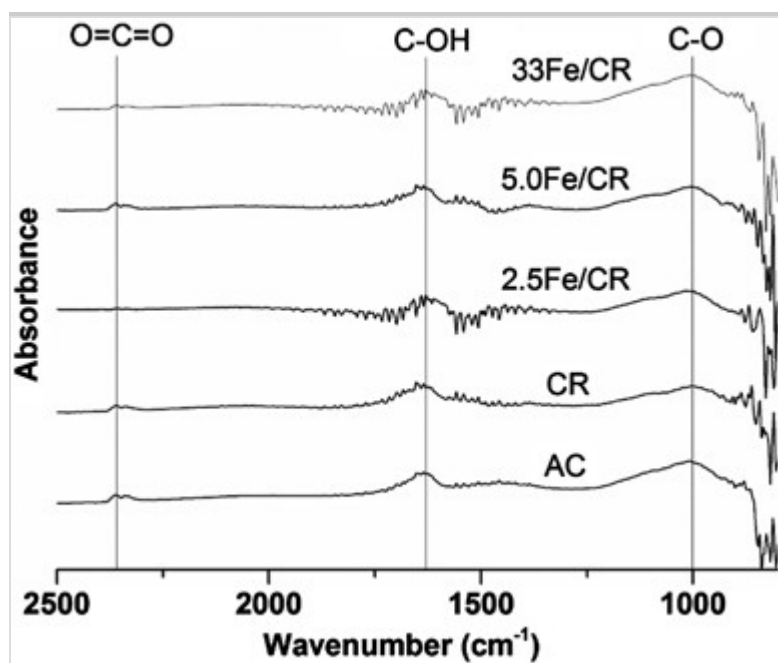


Fig. 2

The infrared spectrum for fresh activated carbon, carbon residue and Fe catalysts at 2500–800 cm^{-1}

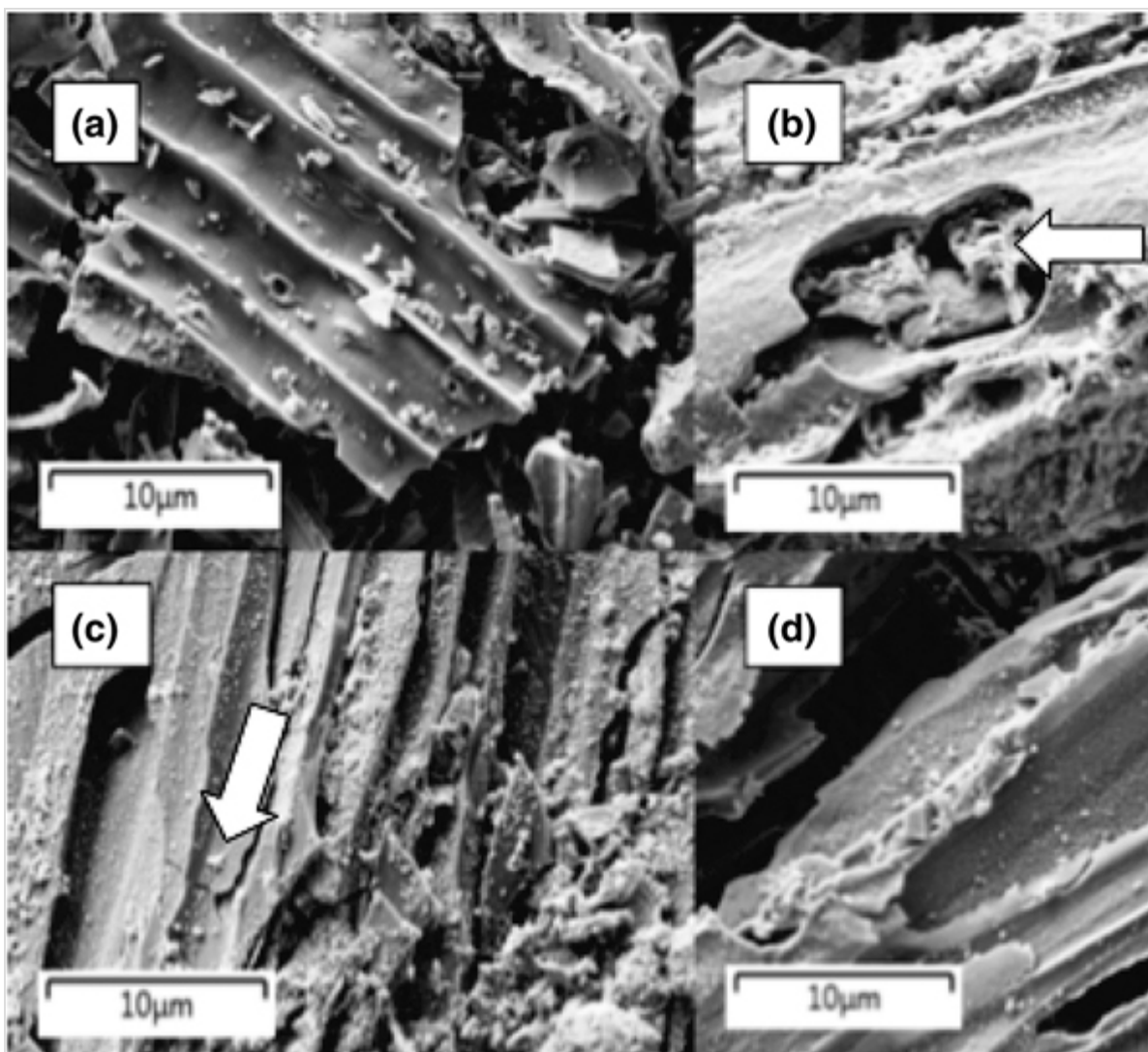


The DRIFTS method was used to qualitatively identify the possible functional groups of the carbon materials. The DRIFTS spectrum of the fresh samples is presented in Fig. 2. The CR and Fe catalysts have spectra comparable to the reference sample, commercial activated carbon. In all samples, a broad peak at around $3420\text{--}3440\text{ cm}^{-1}$ (not shown) was detected. This is the typical stretching of the O-H bond of the surface hydroxyl groups. Furthermore, at wavenumbers $2340\text{--}2360\text{ cm}^{-1}$ the peaks can be attributed to carbon dioxide [62]. Probably the highest peak at around 1640 cm^{-1} is characteristic of adsorbed water [63] while the broad peak at around wavenumber 1000 cm^{-1} is assigned to CO [64].

FESEM analysis was conducted to study the surface morphology of the fresh catalysts. The images obtained from FESEM are shown in Fig. 3, and they were in good agreement with the ICP-OES metal content results (Table 1). The iron particles ($< 1\text{ }\mu\text{m}$) are clearly seen and heterogeneously dispersed on the support in all prepared catalysts. Moreover, the structure of CR was found to be relatively porous and layered.

Fig. 3

SEM images of the fresh catalysts **a** 2.5Fe/CR, **b** 5.0Fe/CR, **c** 33Fe/CR and **d** CR (magnification $\times 5000$). The iron particles are marked with an *arrow*



3.2. Catalytic Wet Peroxide Oxidation of BPA by Different Catalysts

The performance of the as-prepared catalysts was studied in the CWPO reactions that were carried out at 50 °C using 1.5 g L⁻¹ of H₂O₂ as an oxidant. Before the BPA catalytic wet peroxide oxidation runs, an experiment without a catalyst was performed. The non-catalytic test indicated that with hydrogen peroxide 26% of BPA was removed after a 3 h experiment while the pH varied between 5.5 and 8.5 (Table 3). To evaluate the adsorption properties of the prepared catalysts, experiments without the oxidation agent were also conducted. In the adsorption tests, the catalyst amount was 1 g L⁻¹.

The adsorption of BPA onto the catalysts in the absence of H₂O₂ was related to the BET surface area of the samples (Table 1), indicating that

the higher the surface area the higher the removal of BPA by adsorption. The adsorption of BPA varied from 14 to 100%, increasing in the order 33Fe/CR < 5.0Fe/CR < 2.5Fe/CR < CR < AC. The 2.5Fe/CR and 5.0Fe/CR catalysts were found to adsorb 37% and 32% of BPA, respectively, whereas the adsorption of BPA onto the CR was found to be 46%. The adsorption process is known to depend strongly on the pH of the solution [65]. The pH values of the final solution varied from slightly basic (AC, CR, 5.0Fe/CR) to acidic (2.5Fe/CR, 33Fe/CR; Table 2). BPA is found in its molecular form at pH values below 8 [43] where the hydrophobic interactions ($\pi - \pi$ interaction) enhance the adsorption of BPA. The situation changes when the pH value is higher than 8 due to the deprotonation of BPA. The reduction in the adsorption of BPA is partly due to the electrostatic repulsive interactions between the negatively charged carbon surface and the bisphenolate anion [43]. The pH values of the carbon slurries between the 2.5Fe/CR and 5.0Fe/CR catalysts after the heating up period, but just before starting the oxidation reaction (i.e., the H₂O₂ addition) were observed to vary significantly: For the 2.5Fe/CR catalyst, the pH changed from the initial 6 to 3.1 whereas with the 5.0Fe/CR catalyst, the change was in the opposite direction from the initial 6.9–8.6 to 7.3–8.9 (Table 2). The difference between the pH change could be due to the different preparation methods. The 5.0Fe/CR catalyst was prepared at basic conditions whereas for the 2.5Fe/CR catalyst the pH was not controlled. Although the surface properties of the prepared catalysts is not elucidated, it is clear that the 2.5Fe/CR and 5.0Fe/CR catalysts possess different characteristics based on the pH measurement. Therefore, the small difference (5%) observed in the adsorption of BPA between the 2.5Fe/CR and 5.0Fe/CR catalysts might be caused by the difference in the pH as they have similar surface areas. Finally, all catalyst materials yielded much lower adsorption compared to the commercial AC Norit. The high adsorptive properties of carbonaceous materials have been widely presented in the literature [43, 44, 45].

Table 2

The pH change, removal of BPA, TOC conversion and leaching of iron (compared to the initial amount of iron in the prepared Fe catalysts) after 3 h oxidation reaction

Catalyst	pH			BPA removal (%)	TOC- removal (%)	Iron leached (%)
	Initial	Slurry	Final			
Catalyst load 1 g L ⁻¹						
2.5Fe/CR	5.5	3.2	3.1	100	39	3.6
5.0Fe/CR	8.5	8.9	8.6	63	31	-
33Fe/CR	6.9	3.2	3.0	100	51	3.4
AC	8.0	8.8	8.1	100	70	-
CR	6.2	8.4	8.5	65	33	-
Catalyst load 2 g L ⁻¹						
2.5Fe/CR	5.9	3.1	3.0	100	50	14.6
5.0Fe/CR	6.9	7.3	7.8	83	64	0.10
33Fe/CR	5.9	3.0	2.9	100	47	5.1
AC	7.3	5.9	4.9	100	64	-
CR	7.3	6.2	6.3	86	58	-
Operating conditions: c(BPA) = 60 mg L ⁻¹ , c(H ₂ O ₂) = 1.5 g L ⁻¹ , c(catalyst) = 1–2 g L ⁻¹ , T = 50 °C, pH initial						

According to the results, all materials showed similar catalytic activity. The catalysts with the highest load of iron, 2.5Fe/CR and 33Fe/CR, performed the best catalytic activity in terms of BPA removal and TOC conversion with the two catalyst doses (1–2 g L⁻¹). The pH of the effluent for the 2.5Fe/CR and 33Fe/CR catalysts during the CWPO reactions was found to change to more acidic; the final solution pH was around 3, which has been found in many previous studies to be the optimum value for the homogenous Fenton process [34, 54, 56, 66]. The possible explanation for the pH change may be related to the acidic nature of the 2.5Fe/CR and 33Fe/CR catalysts, as can be seen in Table 2. The pH of the carbon slurry changes from around 6 to 3 in both cases. Moreover, the low TOC conversion may also be due to the inefficient decomposition of H₂O₂. The mild operating temperature used in this study (50 °C) may lead to the H₂O₂ decomposition toward non-reactive species such as O₂ or to auto-scavenging reactions if the

decomposition of H_2O_2 occurs very quickly [41]. Furthermore, the leaching of Fe ions is known to be enhanced at low pH values [67, 68], and this can be seen in the case of the 2.5Fe/CR and 33Fe/CR catalysts (Table 2). These results are comparable with the studies reported by Rey et al. and Centi et al. [30, 41]. Therefore, the contribution of homogenous and heterogenous Fenton processes had to be taken into consideration. According to Sabhi et al. [69], the homogenous Fenton process requires $50\text{--}80\text{ mg L}^{-1}$ of iron to maintain the reaction rate at a high level. However, the leached iron concentration found from the effluent was much lower (maximum of 27 mg L^{-1} of iron was observed). Therefore, it might be possible that the CWPO reaction in these operation conditions was mainly heterogeneous and did not go to completion as the iron concentration and the temperature ($50\text{ }^\circ\text{C}$) were relatively low. Moreover, finding the optimum H_2O_2 concentration is vital for the economy of the system. According to the dissolved oxygen measurements, the content of the dissolved oxygen remained steady for all the studied Fe catalysts, and no excess oxygen was available during the experiments, indicating that H_2O_2 was decomposed completely (as presented in Table 3). However, the dissolved oxygen content was significantly higher for CR, and this may indicate that the decomposition of H_2O_2 proceeded mainly through O_2 formation and not through $\text{OH}\cdot$ [34]. Furthermore, the increase in the catalyst dose from 1 to 2 g L^{-1} did not show a significant difference in the BPA removal or TOC conversion for the 2.5Fe/CR and 33Fe/CR catalysts (Table 2). Further, the reference material, commercial AC Norit, was found to remove BPA completely, but this removal was mainly due to the adsorption of BPA, not the catalytic performance of the material.

Table 3

Dissolved oxygen content of BPA samples during the catalytic hydrogen peroxide oxidation experiments

Dissolved O_2 (mg L^{-1})	Non-catalytic	2.5Fe/CR	5.0Fe/CR	33Fe/CR	AC	CR
Initial	9.7	9.7	9.1	9.8	9.9	9.9
	5.8–6.0	5.6–6.2	5.9–6.3	5.8–6.7		

Dissolved O ₂ (mg L ⁻¹)	Non- catalytic	2.5Fe/CR	5.0Fe/CR	33Fe/CR	AC	CR
During H ₂ O ₂ addition					6.2 –8.0	6.8 –14.0
Final	5.9	6.6	5.8	6.8	6.7	9.5

The 5.0Fe/CR and CR catalysts showed similar performance, resulting in approximately 20% higher BPA removal and almost 50% higher TOC conversion when the catalyst load was doubled from the initial 1 g L⁻¹ (Table 2). This phenomenon indicates that increase in the Fe catalyst dose would thus increase the reactive surface area, the amount of iron and hydroxyl radical production that altogether enhance the degradation rate of BPA and TOC conversion [70, 71, 72]. Although the BPA removal was 20–40% lower when compared to the 2.5Fe/CR and 33Fe/CR catalysts, the TOC conversion with the 5.0Fe/CR and CR catalysts was higher when the catalyst dose was increased. The pH values of the carbon slurry before the addition of H₂O₂ for the CR and 5.0Fe/CR catalysts were also around neutral or basic, thus differing from the two other catalysts (Table 2). As can be seen in Table 2, the amount of leached iron from the catalysts into the solution from the 5.0Fe/CR and CR catalysts remained insignificant, and therefore, the oxidation reaction with these catalysts was totally heterogeneous. The iron content in the catalysts has been proposed to be a more significant factor than the specific surface area when the catalytic activity is estimated [58]. As observed, the 5.0Fe/CR and CR catalysts have lower iron content, and therefore, it might explain the lower catalytic activity toward the removal of BPA when compared to the 2.5Fe/CR and 33Fe/CR catalyst. However, the TOC conversion was found to be higher under the neutral to basic conditions. The decomposition of H₂O₂ is accelerated under basic conditions up to 9 [70, 73], and this might have contributed to the more efficient TOC conversion in the present study. In addition, carbon materials catalyze the decomposition of H₂O₂, and especially the basic surface sites of the carbon have been reported to promote faster decomposition of H₂O₂, whereas acidic groups inhibit the reaction [45, 46, 67, 73]. Surface basicity has been

related to the increased efficiency of the CWPO process [42, 74]. Referring to the preparation procedure for the 5.0Fe/CR catalyst and for the basic nature of the CR (pH 9) found in previous studies [57], these results may indicate the presence of more basic surface sites than acidic. Finally, these oxidation results indicate that it is possible to use the biomass-based carbon residue and iron catalyst (5.0Fe/CR) supported on the CR at a wide pH range (5.5–9) as a catalyst in CWPO.

3.3. Kinetic Study

The removal of BPA was further analyzed with a kinetic study that was assumed to be of the first order with respect to its concentration (Figs. 4, 5). Based on this, Eq. (2).

Fig. 4

Time-dependent BPA reduction during catalytic wet peroxide oxidation where the 33Fe/CR catalyst is marked with (*open circle*), 2.5Fe/CR with (*filled triangle*) and 5.0Fe/CR with (*filled square*). Reaction conditions: $c(\text{BPA}) = 60 \text{ mg L}^{-1}$, $c(\text{H}_2\text{O}_2) = 1.5 \text{ g L}^{-1}$, $c(\text{catalyst}) = 1 \text{ g L}^{-1}$, $T = 50 \text{ }^\circ\text{C}$ and at initial pH 5.5–8.5

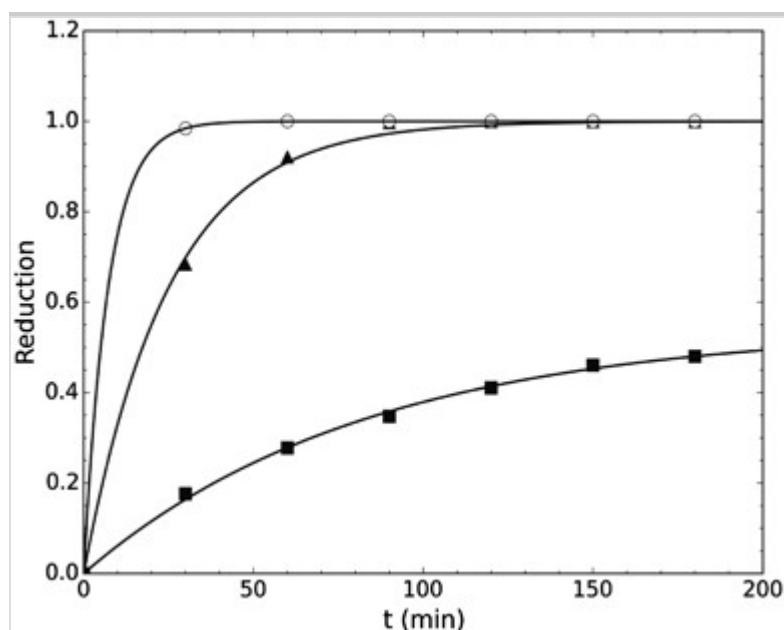
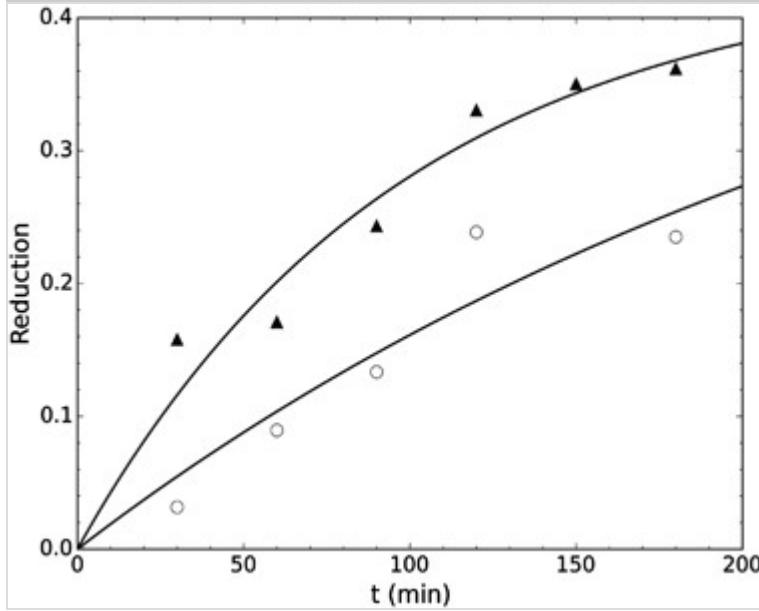


Fig. 5

Time-dependent BPA reduction during catalytic and non-catalytic wet peroxide oxidation where CR support is marked with (*open circle*) and the non-catalytic experiment with (*filled triangle*). Reaction conditions: $c(\text{BPA}) = 60 \text{ mg L}^{-1}$, $c(\text{H}_2\text{O}_2) = 1.5 \text{ g L}^{-1}$, $c(\text{CR}) = 1 \text{ g L}^{-1}$, $T = 50 \text{ }^\circ\text{C}$ and at initial pH 6.2–6.9



$$R(t) = R_{Tot}(1 - e^{-kt}) \quad 2$$

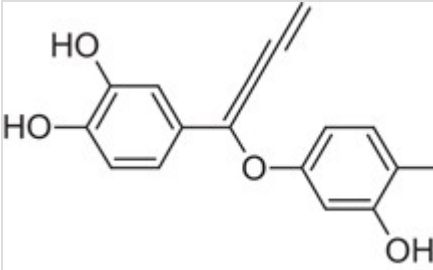
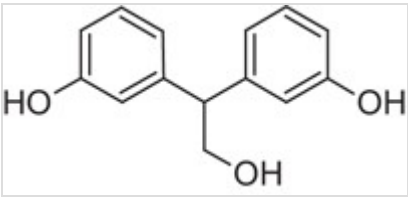
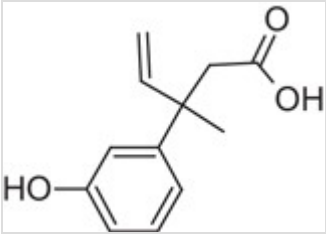
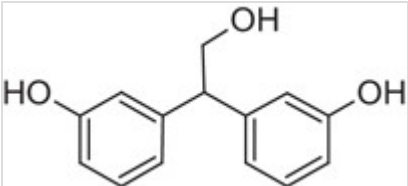
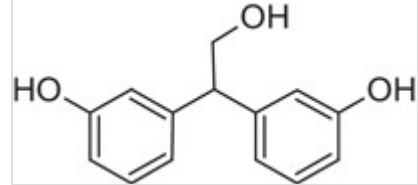
was fitted to the measured data using a standard non-linear least squares algorithm. Total removal R_{Tot} and reaction rate constant k were used as fitting parameters. Goodness of fit was evaluated from the calculated R^2 values and analysis of the residuals. No systematic deviations from the model used in this work were detected for the Fe/CR catalyzed experiments (Fig. 4). The possible rate constants for the 2.5Fe/CR, 5.0Fe/CR and 33Fe/CR catalysts were 2.401, 0.702 and 8.316 h^{-1} , respectively. The reduction rate for BPA by the 33Fe/CR catalyst was about 11.5 times that of the 5.0Fe/CR catalyst. However, as reported in the preceding section, the leaching of iron from the 33Fe/CR catalyst was significant (Table 4) whereas no leaching were observed with the 5.0Fe/CR catalyst. For the experiments with only the CR as the catalyst or no catalyst, the achieved fit was much poorer (Fig. 5), and the rate constants for the CR and non-catalyst experiments were 0.619 and

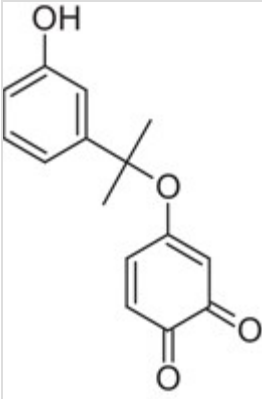

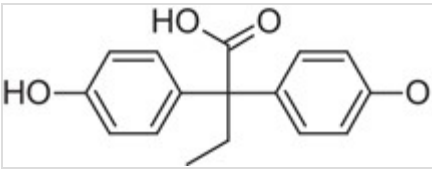
0.218 h⁻¹, respectively. The poor fit was due to the large deviations in the two experiments.

AQ2

Table 4

LC-MS data detected from the oxidized BPA solution catalyzed by 5.0Fe/CR

Compound	Retention time (min)	[M-H]	Formula	Tentative structure
A	1.92	311	C ₁₇ H ₁₂ O ₆	
B	2.16	229	C ₁₄ H ₁₄ O ₃	
C	2.37	205	C ₁₂ H ₁₄ O ₃	
D*	2.57	229	C ₁₄ H ₁₄ O ₃	  <p>structure should be corrected to another structure. The corrected structure is in an attachment (word-file).</p>
E	3.17	257	C ₁₅ H ₁₄ O ₄	

Compound	Retention time (min)	[M-H]	Formula	Tentative structure
				
BPA	3.63	227	C ₁₅ H ₁₆ O ₂	
F	3.72	271	C ₁₆ H ₁₆ O ₄	



3.4. Analysis of by-Products

According to the TOC measurements of the final samples, the removal of organic compounds was not as high as the abatement of BPA during CWPO of BPA (Table 2). For example, in the 5.0Fe/CR catalyzed reaction (catalyst concentration 2 g L⁻¹), the BPA removal was 83% and TOC conversion was 64% while the theoretical TOC conversion should have been higher than 80%. The low TOC conversion refers the formation of by-products during the oxidation reaction. According to the literature several intermediates and by-products have been identified after oxidation of BPA. In the study of Gözmen et al. [75] phenols, catechol, quinones, acetic and formic acids were detected after electro-Fenton treatment of BPA while in the catalytic wet air oxidation of BPA Mezohegyi et al. [76] observed p-hydroxyacetophenone, acetic and formic acids in the final effluent. Therefore, the final samples after the oxidation reactions were analyzed with the liquid chromatography–mass spectrometry (LC-MS) technique. As an example, Fig. 6 presents the chromatogram of the oxidized BPA solution catalyzed by 5.0Fe/CR.

In addition to BPA at the retention time of 3.62 min, six peaks of the products named A–F are observed on the spectrum. The lower retention times of five peaks (A–E) refer to the formation of more polar products than BPA during the oxidation process.

Fig. 6

LC-MS chromatogram of the BPA solution after 3 h of wet peroxide oxidation catalyzed by 5.0Fe/CR 2 g L⁻¹

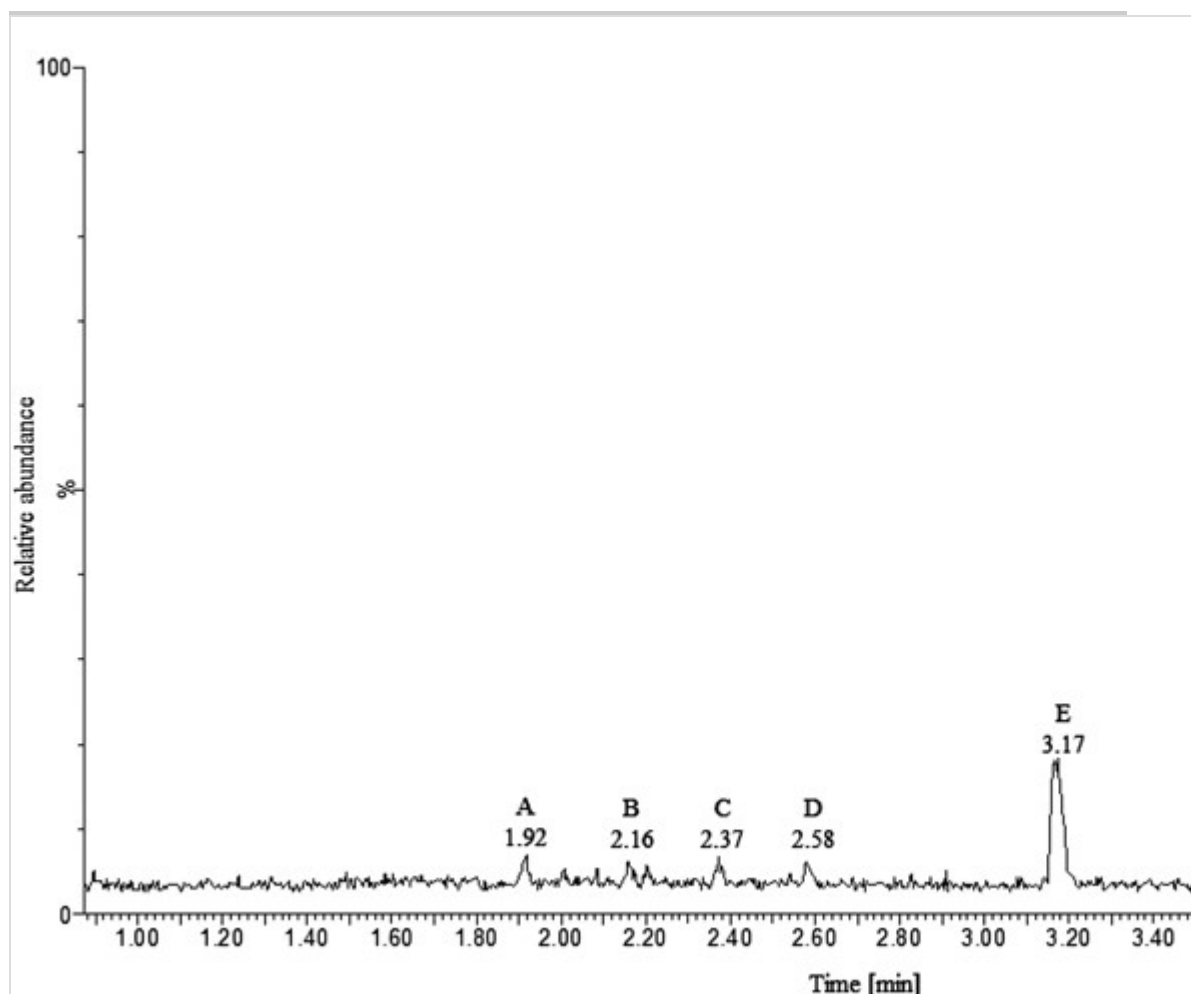


Table 4 lists the [M-1] ions in the negative mode of LC-MS, the detected molecular formulas and the tentative structures of the compounds. Surprisingly, only one of the products, compound C, has a molecular weight lower than BPA and no carboxylic acids were detected. However, this was probably due to the analyzing method because in the study of Mezohegyi et al. [76] acetic and formic acids were analyzed by ion chromatogram. Products B and D have a slightly

higher molecular weight than BPA (230 g mol^{-1}). According to the tentative structures of these compounds, a reaction between oxidized products (methanol and some other intermediate) has probably formed these structures. Products E and F are most obviously formed in the reaction between BPA and the reactive hydrogen radical. Therefore, the Fe/CR catalyzed H_2O_2 oxidation of BPA in to the by-products described in Table 4 happens probably through to the hydroxyl radical ($\cdot\text{OH}$) oxidation which is also proposed in the study of Cleveland et al. [56]. The proposed pathway for Fenton oxidation of BPA is described e.g. in the study of Poerschmann et al. [21] and Luo et al. [77]. Moreover, similar by-products have been identified in several studies [21, 78, 79, 80] However, the chromatogram shows (Fig. 6) that the relative abundance of compounds A–D is much lower than the BPA concentration, which causes inaccurate results. Therefore, the proposed molecular structures of these compounds are only tentative. The possible toxicity of the identified by-products was examined from the literature. Due to the phenolic structure of all by-products they may be estrogenic active [81]. However, Ye et al. [82] have been reported that the catechol structure of BPA has three times lower estrogenic activity than that of BPA in MCF-7 cells. Therefore, the compound A with the catechol structure could have lower estrogenic activity than the BPA. Moreover, in the study of Kitamura et al. [81] the estrogenic activity of BPA-related compounds was studied in both MCF-7 cells and ovariectomized mice. They observed that hydroxylated propane groups decreased the estrogenic activity i.e. isomers B and D with propane bridge groups could be less toxic than BPA. Furthermore, quinone derivate of BPA (compound E) could probably be more toxic than BPA itself due to the potential mutagenicity of such compounds [83, 84].

3.5. Characterization of Used Catalysts

Table 5 summarizes the iron content, the BET surface area, as well as the relative pore size distribution of the catalysts. Compared to the fresh catalysts (Table 1), the Fe content of the 2.5Fe/CR and 5.0Fe/CR catalysts remained stable, although the first showed significant leaching of iron in the liquid phase after the CWPO reaction. The used preparation method (multiple impregnation under acidic conditions) for the 2.5Fe/CR might have had a negative impact for the iron

impregnation. The longer impregnation time have been attributed to reduce the iron impregnation due to the exchange of iron ions by protons (H^+) under acidic conditions [85, 86]. Furthermore, during the impregnation there might have been competition between the adsorbed iron ions and aqueous iron ions which lowers the iron impregnation. The BET surface area remained almost unchanged, and the increase observed with the 33Fe/CR catalyst is due to the iron leaching (Table 2). These results are somewhat ambiguous in the case of the 2.5Fe/CR catalyst because the results for the BET surface area would imply that iron would have remained (i.e., the area did not change) rather than it being leached. Therefore, it could be hypothesized because the used CR support was non-homogenous material (see Fig. 3), not only the bulk content of iron but also the amount of leached iron varied. Thus, during the oxidation reaction the H_2O_2 dissolved the organic carbon from the CR support and thus may have released iron from the bulk content easier. This hypothesis is supported by the ICP-OES result, from which it can be observed that the iron content was reduced when the used CR (Table 5) is compared to fresh CR (Table 1). In the case of AC and CR, the surface area was decreased which might be due to the pore blockage caused by agglomeration of pollutants [87] and/or it might be the result of the adsorbed BPA on the surface. Micro- and mesopores are the most effective for removing organic pollutants [88]. The 2.5Fe/CR and CR catalysts had the largest volumes of pores when the micro- and mesopore volumes were combined (83.6 and 83.5%, respectively) whereas AC had the smallest (27.3%). The micro- and mesopore volumes increased almost every used catalyst compared to the pore volumes of the fresh catalysts (Table 1). For the 2.5Fe/CR and 5.0Fe/CR and CR catalysts, the increase was less than 2% while the highest increase was found for AC (7.5%) and was 4% for the 33Fe/CR catalyst. This might be due to the leaching of iron (and other compounds) from the catalyst active sites during the experiments. The total pore volumes remained steady for the 2.5Fe/CR and 5.0Fe/CR catalysts and for the CR, while a 31 and 25% decrease was found in AC and 33Fe/CR, respectively. Again, this might be due to the pore blockage of these materials.

Table 5

Iron content, BET surface area, total pore volume and relative distribution of the micro-, meso- and macropores of used catalysts

Catalyst	Fe-content (%)	BET surface area (m ² g ⁻¹)	Total pore volume (cm ³ g ⁻¹)	V _{Micro} (%)	V _{Meso} (%)	V _{Makro} (%)
2.5Fe/CR	4.8	64.0	0.093	5.40	79.5	15.1
5.0Fe/CR	5.0	67.0	0.096	7.30	79.2	13.5
33Fe/CR	—	55.1	0.098	5.10	68.4	26.5
AC	0.21	721	0.298	20.8	69.8	9.40
CR	0.06	58.8	0.100	5.00	81.0	14.0

Figure 7 presents X-ray diffractograms for the used catalysts. Compared to the diffractograms of the fresh CR support and catalysts (Fig. 1), the X-ray diffractograms for the CR, 2.5Fe/CR and 33Fe/CR catalysts show no significant changes. This suggests that the support material and these catalysts are stable materials. The reflections obtained for the 5.0Fe/CR catalyst at 2θ 29.3°, 31.7° and 36.6° correspond to Fe₃O₄ (JCPDS: 00-003-0863) and indicate that NaCl was leached during the CWPO process. The EDS analysis confirmed this result: No sodium or chloride was detected in the used 5.0Fe/CR catalyst. In addition, the presence of iron (7.55 wt%) was detected. Figure 8 presents the FESEM images of the used catalysts, and they were in good agreement with the results presented. Similarly, the porous and layered structure was clearly seen as well as the heterogeneously dispersed iron particles ($<<1\ \mu\text{m}$) when compared to the FESEM images obtained for the fresh catalyst (Fig. 3).

Fig. 7

X-ray diffractograms of the used carbon residue support (1) and Fe catalysts (2–4). (*plus*) JCPDS:01-078-3262 (CaCO₃); (*asterisk*) JCPDS: 00-003-0863 (Fe₃O₄); (*double quotes*) JCPDS: 01-089-0597 (Fe₂O₃); (*hash*) JCPDS: 04-015-9580 (Fe₂O₃)

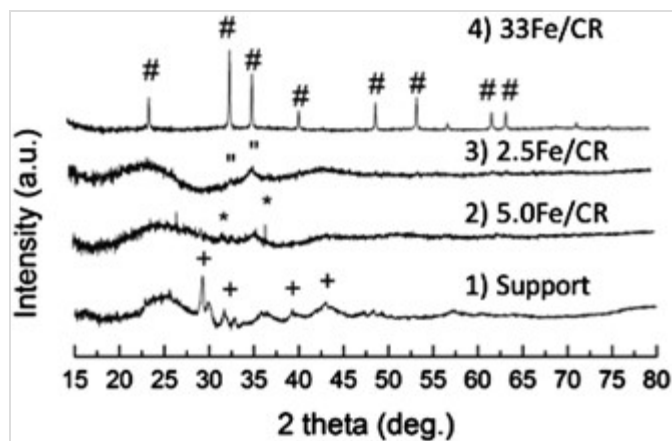
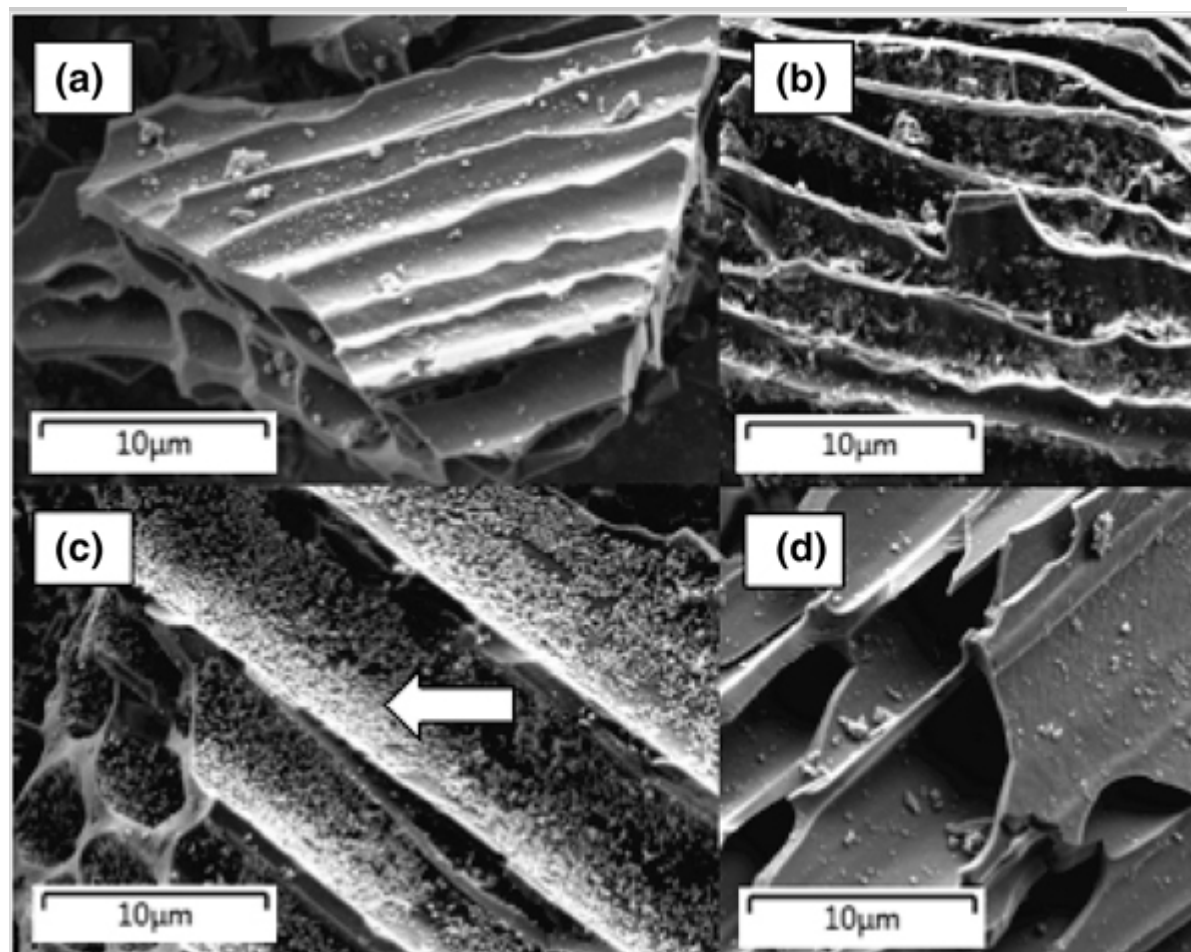


Fig. 8

SEM images of used, **a** 2.5Fe/CR, **b** 5.0Fe/CR, **c** 33Fe/CR and **d** CR catalysts (magnification $\times 5000$). The porous structure (**b**) and the iron particles (**c**) are marked with an *arrow*



4. Conclusions

Three iron catalysts were prepared by using a biomass-based CR as the support. One Fe catalyst (2.5Fe/CR) was prepared with incipient wet impregnation and two Fe catalysts (5.0Fe/CR and 33Fe/CR) with wet impregnation with an iron chloride solution. The degradation of BPA was studied using the prepared Fe catalysts in CWPO experiments. The iron impregnation to the CR support decreased the BET surface area values that varied between the catalysts from 17 to 66 m² g⁻¹. For the CR support, the BET surface area value was 91 m² g⁻¹. The catalyst 5.0Fe/CR was concluded to be the best catalyst. It was found to be the most stable catalyst as a result of negligible iron leaching during the 3 h experiment. In addition, the 5.0Fe/CR catalyst showed lower oxidation activity than 2.5Fe/CR and 33Fe/CR, but the TOC conversion were 15–20% higher. These oxidation results indicate that the biomass-based carbon residue-supported 5.0Fe/CR can be used as a catalyst, and pure carbon residue can be used as a catalyst in CWPO in the degradation of BPA. With this material, it is possible to operate up to a 5.5 pH value close to 9 using 5.0Fe/CR and CR as catalysts.

AQ3

Acknowledgements

The authors gratefully acknowledge the Academy of Finland for providing research funding, AOPI project (263397) within the research program for Sustainable Governance of Aquatic Resources (AKVA). The Tauno Tönning Foundation is gratefully acknowledged for its financial support. The authors would like to thank PhD Henrik Romar for the BET, pore size and pore volume measurements and Jaakko Pulkkinen (AAS) and Tuomas Vähätiitto (TOC). We also thank the staff at TraceElement Laboratory at the University of Oulu for their assistance with the elementary analysis. Lotta Hekkala and Aleksanteri Nikula are acknowledged for their support during the laboratory work.

References

1. Selvaraj KK, Shanmugam G, Sampath S, Joakim Larsson DG, Ramaswamy BR (2014) *Ecotoxicol Environ Saf* 99:13–20

2. Belfroid A, Van Velzen M, Van der Horst B, Vethaak D (2002) *Chemosphere* 49:97–103
3. Väitalo P, Perkola N, Seiler T, Sillanpää M, Kuckelkorn J, Mikola A, Hollert H, Schultz E (2016) *Water Res* 88:740–749
4. Campbell CG, Borglin SE, Green FB, Grayson A, Wozel E, Stringfellow WT (2006) *Chemosphere* 65:1265–1280
5. Nelson J, Bishay F, van Roodselaar A, Ikonomou M, Law FCP (2007) *Sci Total Environ* 374:80–90
6. Jurado A, Vázquez-Suñé E, Carrera J, López de Alda M, Pujades E, Barceló D (2012) *Sci Total Environ* 440:82–94
7. Luo Y, Guo W, Ngo HH, Nghiem LD, Hai FI, Zhang J, Liang S, Wang XC (2014) *Sci Total Environ* 473–474:619–641
8. Gültekin I, Ince NH (2007) *J Environ Manage* 85:816–832
9. United States Environmental Protection Agency. (1998). Endocrine disruptor testing and screening advisory committee (EDSTAC). Final report. Washington, DC, US
10. Yamamoto T, Yasuhara A, Shiraishi H, Nakasugi O (2001) *Chemosphere* 42:415–418
11. Ying G, Kookana RS, Kumar A, Mortimer M (2009) *Sci Total Environ* 407:5147–5155
12. PlasticsEurope (2007) Applications of bisphenol A. Polycarbonate/bisphenol A (BPA) groups of industry association PlasticsEurope. <http://www.bisphenol-a-europe.org/uploads/applications%20of%20BPA%20Sept%2008.pdf>
13. Staples CA, Dorn PB, Klecka GM, O’Block ST, Harris LR (1998) *Chemosphere* 36:2149–2173

14. Seachrist DD, Bonk KW, Ho S, Prins GS, Soto AM, Keri RA (2016) *Reprod Toxicol* 59:167–182
15. Levy G, Lutz I, Krüger A, Kloas W (2004) *Environ Res* 94:102–111
16. Markey CM, Coombs MA, Sonnenschein C, Soto AM (2003) *Evol Dev* 5:67–75
17. Richter CA, Birnbaum LS, Farabollini F, Newbold RR, Rubin BS, Talsness CE, Vandenberg JG, Walser-Kuntz DR, vom Saal FS (2007) *Reprod Toxicol* 24:199–224
18. Li G, Lu Y, Lu C, Zhu M, Zhai C, Du Y, Yang P (2015) *J Hazard Mater* 294:201–208
19. Ioan I, Wilson S, Lundanes E, Neculai A (2007) *J Hazard Mater* 142:555–558
20. Katsumata H, Kawabe S, Kaneco S, Suzuki T, Ohta K (2004) *J Photochem Photobiol A Chem* 162:297–305
21. Poerschmann J, Trommler U, Górecki T (2010) *Chemosphere* 79:975–986
22. Kwon J, Lee B (2015) *Chem Eng Res Design* 104:519–529
23. Cesaro A, Naddeao V, Belgiorno V (2013) *J Bioremed Biodeg* 4:208
24. Neyens E, Baeyens J (2003) *J Hazard Mater* 98:33–50
25. Huling SG, Kan E, Wingo C (2009) *Appl Catal B Environ* 89:651–658
26. Perathoner S, Centi G (2005) *Top Catal* 33:207–224

27. Li J, Gu J, Li H, Liang Y, Hao Y, Sun X, Wang L (2010) *Microporous Mesoporous Mater* 128:144–149
28. Gomes HT, Miranda SM, Sampaio MJ, Silva AMT, Faria JL (2010) *Catal Today* 151:153–158
29. Gomes HT, Miranda SM, Sampaio MJ, Figueiredo JL, Silva AMT, Faria JL (2011) *Appl Catal B Environ* 106:390–397
30. Centi G, Perathoner S, Torre T, Verduna MG (2000) *Catal Today* 55:61–69
31. Melero JA, Martínez F, Botas JA, Molina R, Pariente MI (2009) *Water Res* 43:4010–4018
32. Fenton HJH (1894) *J Chem Soc* 65:899–910
33. Pignatello JJ, Oliveros E, MacKay A (2006) *Crit Rev Environ Sci Technol* 36:1–84
34. Zazo JA, Casas JA, Mohedano AF, Rodríguez JJ (2006) *Appl Catal B Environ* 65:261–268
35. Messele SA, Soares OSGP, Órfão JJM, Stüber F, Bengoa C, Fortuny A, Fabregat A, Font J (2014) *Appl Catal B Environ* 154–155:329–338
36. Navalon S, Alvaro M, Garcia H (2010) *Appl Catal B Environ* 99:1–26
37. Zhang X, Ding Y, Tang H, Han X, Zhu L, Wang N (2014) *Chem Eng J* 236:251–262
38. Ramirez JH, Costa CA, Madeira LM, Mata G, Vicente MA, Rojas-Cervantes ML, López-Peinado AJ, Martín-Aranda RM (2007) *Appl Catal B* 71:44–56

39. Gemeay AH, Mansour IA, El-Sharkawy RG, Zaki AB (2003) *J Mol Catal A Chem* 193:109–120
40. Rodríguez-Reinoso F (1998) *Carbon* 36:159–175
41. Rey A, Faraldos M, Casas JA, Zazo JA, Bahamonde A, Rodríguez JJ (2009) *Appl Catal B Environ* 86:69–77
42. Ribeiro AR, Nunes OC, Pereira MFR, Silva AMT (2015) *Environ Int* 75:33–51
43. Bautista-Toledo I, Ferro-García MA, Rivera-Utrilla J, Moreno-Castilla C, Fernández FJV (2005) *Environ Sci Technol* 39:6246–6250
44. Chang Q, Lin W, Ying W (2010) *J Hazard Mater* 184:515–522
45. Santos VP, Pereira MFR, Faria PCC, Órfão JJM (2009) *J Hazard Mater* 162:736–742
46. Oliveira LCA, Silva CN, Yoshida MI, Lago RM (2004) *Carbon* 42:2279–2284
47. The European parliament and the council of the European Union (2008). Directive 2008/98/ec., 2008. <http://eur-lex.europa.eu/legal-content/EN/TXT/?qid=1472559001854&uri=CELEX:32008L0098>
48. Martínez ML, Torres MM, Guzmán CA, Maestri DM (2006) *Ind Crops Prod* 23:23–28
49. Jagtoyen M, Derbyshire F (1998) *Carbon* 36:1085–1097
50. Tancredi N, Medero N, Möller F, Píriz J, Plada C, Cordero T (2004) *J Colloid Interface Sci* 279:357–363
51. Ribeiro RS, Silva AMT, Figueiredo JL, Faria JL, Gomes HT (2016) *Appl Catal B* 187:428–460

52. Choi J, Kim T, Choo K, Sung J, Saidutta MB, Ryu S, Song S, Ramachandra B, Rhee Y (2005) *Appl Catal A Gen* 290:1–8
53. Zhong Y, Li G, Zhu L, Yan Y, Wu G, Hu C (2007) *J Mol Catal A* 272:169–173
54. Ramirez JH, Maldonado-Hódar FJ, Pérez-Cadenas AF, Moreno-Castilla C, Costa CA, Madeira LM (2007) *Appl Catal B Environ* 75:312–323
55. Rodríguez A, Ovejero G, Sotelo JL, Mestanza M, García J (2010) *Ind Eng Chem Res* 49:498–505
56. Cleveland V, Bingham J, Kan E (2014) *Sep Purif Technol* 133:388–395
57. Kilpimaa S, Kuokkanen T, Lassi U (2013) *BioResources* 8:1011–1027
58. Domínguez CM, Quintanilla A, Ocón P, Casas JA, Rodriguez JJ (2013) *Carbon* 60:76–83
59. Dastgheib SA, Ren J, Rostam-Abadi M, Chang R (2014) *Appl Surf Sci* 290:92–101
60. Rey A, Faraldos M, Bahamonde A, Casas JA, Zazo JA, Rodríguez JJ (2008) *Ind Eng Chem Res* 47:8166–8174
61. Tsoncheva T, Velinov N, Ivanova R, Stoycheva I, Tsyntsarski B, Spassova I, Paneva D, Issa G, Kovacheva D, Genova I (2015) *Microporous Mesoporous Mater* 217:87–95
62. Williams DH, F. I (1995) *Spectroscopic methods in organic chemistry*, 5th edn. McGraw-Hill publishing, Berkshire, pp 41–45
63. Mao W, Ma H, Wang B (2009) *J Hazard Mater* 167:707–712

64. Romanos J, Beckner M, Stalla D, Tekeei A, Suppes G, Jalisatgi S, Lee M, Hawthorne F, Robertson JD, Firlej L (2013) *Carbon* 54:208–214
65. Radovic LR, Mureno-Castilla C, Rivera-Utrilla J. (2001). Carbon materials as adsorbents in aqueous solutions. In Marcel-Dekker (ed), *Chemistry and physics of carbon*, Marcel-Dekker, New York, pp. 227–405
66. Catrinescu C, Teodosiu C, Macoveanu M, Miehe-Brendlé J, Le Dred R (2003) *Water Res* 37:1154–1160
67. Lücking F, Köser H, Jank M, Ritter A (1998) *Water Res* 32:2607–2614
68. Timofeeva MN, Khankhasaeva ST, Badmaeva SV, Chuvilin AL, Burgina EB, Ayupov AB, Panchenko VN, Kulikova AV (2005) *Appl Catal B* 59:243–248
69. Sabhi S, Kiwi J (2001) *Water Res* 35:1994–2002
70. Huang YQ, Wong CKC, Zheng JS, Bouwman H, Barra R, Wahlström B, Neretin L, Wong MH (2012) *Environ Int* 42:91–99
71. Hermanek M, Zboril R, Medrik I, Pechousek J, Gregor C (2007) *J Am Chem Soc* 129:10929–10936
72. Sun S, Lemley AT (2011) *J Mol Catal A Chem* 349:71–79
73. Khalil LB, Girgis BS, Tawfik TAM (2001) *J Chem Technol Biotechnol* 76:1132–1140
74. Rey A, Zazo JA, Casas JA, Bahamonde A, Rodriguez JJ (2011) *Appl Catal A Gen* 402:146–155
75. Gözmen B, Oturan MA, Oturan N, Erbatur O (2003) *Environ Sci Technol* 37:3716–3723

76. Mezohegyi G, Erjavec B, Kaplan R, Pintar A (2013) *Ind Eng Chem Res* 52:9301–9307
77. Luo S, Yang S, Sun C, Wang X (2011) *Water Res* 45:1519–1528
78. Chakma S, Moholkar VS (2014) *Ind Eng Chem Res* 53:6855–6865
79. Deborde M, Rabouan S, Mazellier P, Duguet J, Legube B (2008) *Water Res* 42:4299–4308
80. Kondrakov AO, Ignatev AN, Frimmel FH, Bräse S, Horn H, Revelsky AI (2014) *Appl Catal B Environ* 160–161:106–114
81. Kitamura S, Suzuki T, Sanoh S, Kohta R, Jinno N, Sugihara K, Yoshihara S, Fujimoto N, Watanabe H, Ohta S (2005) *Toxicol Sci* 84:249–259
82. Ye X, Zhou X, Needham LL, Calafat AM (2011) *Anal Bioanal Chem* 399:1071–1079
83. Edmonds JS, Nomachi M, Terasaki M, Morita M, Skelton BW, White AH (2004) *Biochem Biophys Res Commun* 319:556–561
84. Atkinson A, Roy D (1995) *Biochem Biophys Res Commun* 210:424–433
85. Park H, Koduru JR, Choo K, Lee B (2015) *J Hazard Mater* 286:315–324
86. Koduru JR, Lingamdinne LP, Singh J, Choo K- (2016) *Process Saf Environ Prot* 103:87–96
87. Lu X, Jiang J, Sun K, Xie X, Hu Y (2012) *Appl Surf Sci* 258:8247–8252

88. Li Q, Snoeyink VL, Mariñas BJ, Campos C (2003) Water Res
37:4863–4872